HOKKAIDO UNIVERSITY

Title	Changes in AMPK alpha and Ubiquitin Ligases in Myocyte Reverse Remodeling after Surgical Ventricular Reconstruction in rats with ischemic cardiomyopathy
Author(s)	Shingu, Yasushige; Hieda, Tetsuya; Sugimoto, Satoshi et al.
Citation	Molecular Biology Reports, 49(6), 4885-4892 https://doi.org/10.1007/s11033-022-07347-8
Issue Date	2022-06-01
Doc URL	https://hdl.handle.net/2115/89789
Rights	This version of the article has been accepted for publication, after peer review (when applicable) and is subject to Springer Nature's AM terms of use, but is not the Version of Record and does not reflect post-acceptance improvements, or any corrections. The Version of Record is available online at: http://dx.doi.org/10.1007/s11033-022-07347-8
Type	journal article
File Information	MBR 49(6) 4885-4892.pdf

Hokkaido University Collection of Scholarly and Academic Papers : HUSCAP

Changes in AMPKα and Ubiquitin Ligases in Myocyte Reverse Remodeling after Surgical Ventricular Reconstruction in Rats with Ischemic Cardiomyopathy

Yasushige Shingu[a*], Tetsuya Hieda[a], Satoshi Sugimoto[b], Hidetsugu Asai[c], Tomoji Yamakawa[d], and Satoru Wakasa[a]

[a]Department of Cardiovascular and Thoracic Surgery, Faculty of Medicine and Graduate School of Medicine, Hokkaido University, Sapporo, Japan
[b]Department of Cardiovascular Surgery, Obihiro Kosei Hospital, Obihiro, Japan
[c]Department of Cardiovascular Surgery, Hokkaido Medical Center for Child Health and Rehabilitation, Sapporo, Japan
[d]Department of Cardiovascular Surgery, Kinikyo Chuo Hospital, Sapporo, Japan

[*]**Corresponding author:**
Yasushige Shingu
Department of Cardiovascular and Thoracic Surgery
Faculty of Medicine and Graduate School of Medicine, Hokkaido University
Kita 15, Nishi 7, Kitaku, Sapporo, 060-8638
Japan
Tel: +81-11-716-1161 (ext. 6042)
Fax: +81-11-706-7612
Email: shingu@huhp.hokudai.ac.jp

Key words: Atrogin-1, Murf-1, AMPKα, myocyte reverse remodeling, surgical ventricular reconstruction

Acknowledgments

We would like to thank Editage for English language editing.

Abstract

Background: The change in myocardial protein degradation systems after ventricular unloading has been unknown. We aimed to evaluate the anti-hypertrophic protein adenosine monophosphate-activated protein kinase (AMPK) and two major protein degradation systems (ubiquitin proteasome system and autophagy) in a model of surgical ventricular reconstruction (SVR) in rats with ischemic cardiomyopathy.

Methods and Results: Rats were randomized into the following groups: sham/sham (control group), myocardial infarction (MI)/sham (sham group) and MI/SVR (SVR group), with an interval of 4 weeks. Two (early, n=5 for each) and 28 days (late, n=5 for each) after SVR, ventricular size, and wall stress were assessed. Myocyte area, protein expression of AMPKα and autophagy markers, and gene expression of ubiquitin ligases (*Atrogin-1* and *Murf-1*) were evaluated in the late phase. In the early phase, left ventricular dimensions and wall stress were smaller in the SVR group than in the sham group, whereas they were comparable in the late period. Myocyte area in the SVR group was reduced to the value in the control group, while it was larger in the sham group than in the control group. Total-AMPKα, p-AMPKα, and AMPKα phosphorylation rates were higher, and *Atrogin-1* and *Murf-1* were lower in the SVR group than in the sham group, while the autophagy markers were not different between the groups. p-AMPKα had strong negative correlations with myocyte area, *Atrogin-1*, and *Murf-1*.

Conclusions: In myocyte reverse remodeling after SVR, AMPKα phosphorylation increased in association with reduced gene expression of ubiquitin ligases.

1. Introduction

Excessive myocyte hypertrophy is associated with an increased risk of sudden cardiac death and heart failure. Therefore, the development of novel therapeutic interventions to induce myocyte reverse remodeling is necessary for the treatment of heart diseases [1]. However, the mechanism of myocyte reverse remodeling and change in myocardial protein degradation systems after left ventricular (LV) unloading have been unknown.

Adenosine monophosphate-activated protein kinase (AMPK) has been reported to be not only a central regulator of energy homeostasis but also have antihypertrophic effects by decreasing protein synthesis [2]. AMPK is a heterotrimeric complex composed of a catalytic α subunit and regulatory β and γ subunits. Phosphorylation of AMPKα at Thr172 has been reported to be essential for AMPKα activation, which inhibits cardiac hypertrophy due to pressure overload [3]. Two major protein degradation systems, the ubiquitin proteasome system (UPS) and autophagy, are also important for myocyte remodeling in various heart diseases. The UPS functions by labeling specific proteins with ubiquitin molecules, which are recognized and degraded by proteasomes. Many intracellular short-lived proteins are selectively degraded by the ubiquitinproteasome. Autophagy degrades proteins and organelles via a double-membrane vacuole, the autophagosome, which is delivered to and fuses with a lysosome [4].

Surgical ventricular reconstruction (SVR) is a common surgical LV-volume unloading procedure used for a dilated heart with an akinetic scar. SVR has three effects on the LV: LV unloading (wall stress reduction), exclusion of non-contractile lesions, and restoration of an elliptical LV shape [5]. Although we previously reported that autophagy

plays an important role in LV redilation late after SVR, we did not focus on the relationship between myocyte reverse remodeling and AMPKα [6]. In the present study, we aimed to evaluate AMPKα, UPS, and autophagy in a model of LV unloading by SVR in rats with ischemic cardiomyopathy.

2. Materials and Methods

2.1 Experimental protocol

Figure 1a shows the experimental protocol. Fifteen 10-week-old male Sprague-Dawley rats weighing 325–368 g were randomized into the following three groups: sham/sham (control group), myocardial infarction (MI)/sham (sham group), and MI/SVR (SVR group), with an interval of 28 days. MI and SVR were performed as previously reported [6]. Briefly, in MI, following a left lateral thoracotomy under ventilation, the proximal left anterior descending artery was ligated with 7-0 polypropylene sutures (Ethicon, Somerville, NJ, USA). In SVR, a horizontal sternotomy was performed 28 days after MI, and plication of the akinetic scar area was conducted using three mattress sutures with pledgetted 6-0 polypropylene (Ethicon). The sham operation was a sternotomy without SVR. Rats were anesthetized with intramuscular ketamine (90 mg/kg) and xylazine (10 mg/kg) for MI and SVR. Rats were euthanized 28 days after SVR (or sham) by intraperitoneal injection of sodium pentobarbitone (150 mg/kg). The excised hearts stopped beating immediately after being soaked in ice-cold phosphate-buffered saline. Histological examination, quantitative real-time reverse transcription polymerase chain reaction (RT-PCR), and western blotting of the

left ventricular myocardium were performed. The other 15 rats were used to evaluate the early effects of SVR (2 days) on cardiac function.

2.2 Cardiac functional assessment

Transthoracic echocardiography was performed using a SONOS 5500 ultrasound system with a 12-MHz phased-array transducer (Philips Medical Systems, Andover, MA, USA). M-mode images were recorded in the long-axis view of the LV for the following parameters: LV end-diastolic and end-systolic dimensions (LVDd and LVDs), fractional shortening (FS), and LV posterior wall thickness in systole (PWTs). For Millar catheter examination, a 1.4-Fr micromanometer-tipped catheter (Millar, Houston, TX, USA) was inserted into the ascending aorta and LV through the right carotid artery. The pressure data were recorded in PowerLab (ADInstruments, Dunedin, NZ) and analyzed using LabChart (ADInstruments). The systolic wall stress was calculated as $0.333 \times LVSP \times LVDs/(PWTs \times [1+PWTs/LVDs])$ ($kdynes/cm^2$), where LVSP represents the LV peak systolic pressure [7]. Infarct size was estimated by scar ratio, which was calculated as the circumferential of the akinetic endocardium divided by that of the total endocardium at the papillary muscle level by a short-axis view.

2.3 Histological examination

The mid walls of the LV were fixed in 3.5% paraformaldehyde in phosphate-buffered saline, embedded in paraffin, and sectioned at 5-μm intervals. Hematoxylin-eosin and Masson's trichrome staining were performed using standard procedures at the mid-ventricular level.

Approximately 100 randomly chosen oval-shaped cardiomyocytes with a nucleus in the septal lesion of hematoxylin-eosin-stained sections were analyzed to measure the cardiomyocyte area (μm^2) using ImageJ software (http://rsb.info.nih.gov/ij/) (NIH, Bethesda, Maryland). The percentage of the fibrotic area compared to the whole tissue area was calculated using Masson's trichrome-stained sections. Approximately 10 randomly chosen frames in the septal lesions were analyzed using ImageJ (NIH).

2.4 Western blotting

The protein expression of AMPKα, AKT, autophagy markers, and ubiquitin was assessed by western blotting using the viable LV myocardium. While AMPK is a well-known cellular energy sensor, it has also been reported to have various downstream targets and inhibit protein synthesis and muscle growth [8]. AMPKα activation was measured as phospho-AMPKα (p-AMPKα) relative to total AMPKα. AKT also plays a critical role in cell growth by directly phosphorylating mTOR in a rapamycin-sensitive complex raptor, termed TORC1 [9]. Autophagy was evaluated using the two markers. Upon activation of autophagy, microtubule-associated protein light chain 3 (LC3)-I (cytosolic form) converts to LC3-II (membrane-bound lipidated form), which subsequently attaches to the autophagosomal membrane. Therefore, LC3-II levels reflect the number of autophagosomes. In contrast, p62 is selectively incorporated into autophagosomes through direct binding to LC3 and is degraded by autophagy; the expression levels of p62 decrease after autophagic activation [10].

A semi-dry western blot apparatus (Mini-PROTEAN Tetra Cell, BIO-RAD, CA, USA)

was used for western blotting. After sodium dodecyl sulfate-polyacrylamide gel electrophoresis (12% Mini-PROTEANTGX^{TM}, BIO-RAD, CA, USA), the proteins were blotted onto polyvinylidene difluoride membranes and incubated with primary antibodies (AKT, p-AKT [Ser473], AMPKα, p-AMPKα [Thr172], glyceraldehyde-3-phosphate dehydrogenase [GAPDH], p62/SQSTM1, ubiquitin: Cell Signaling, MA, USA; anti-LC3B, Abcam, Cambridge, UK) and secondary antibodies (anti-rabbit IgG, Cell Signaling). The bands were semi-quantified by chemiluminescence using JustTLC (Sweday, Sodra Sandby, Sweden). Protein expression was normalized to GAPDH as a loading control. For ubiquitin, the membrane was dyed with naphthol blue black solution to normalize the band intensity.

2.5 RT-PCR

The gene expression of ubiquitin ligases was evaluated by RT-PCR using the viable LV myocardium. UPS is a major protein degradation system. Proteins are targeted for degradation by the UPS by covalent attachment of a chain of ubiquitin molecules. The multistep pathway involves the activation of the small protein ubiquitin by an enzyme, E1, which then transfers the highly reactive ubiquitin to one of the cell's ubiquitin-conjugating enzymes, E2s. A ubiquitin protein ligase, E3, then binds to the protein substrate and ubiquitin-E2 and catalyzes the formation of a chain of ubiquitins on the protein [11]. The gene expression of muscle-specific ubiquitin ligases E3, *Atrogin-1*, and *Murf-1* was assessed by RT-PCR. Both *Atrogin-1* and *Murf-1* have been extensively studied in atrophy of the skeletal muscles and termed "atrogens."

Myocardial mRNA was isolated from frozen tissue samples using a High Pure RNA

Tissue Kit (Roche, Penzberg, Germany). mRNA was reverse transcribed into cDNA using a Transcriptor First Strand cDNA Synthesis Kit (Roche). RT-PCR was performed with FastStart Essential DNA Probes Master (Roche) and RealTime ready assay (Roche Assay ID, 505442 for *Atrogin-1*; 505441 for *Murf-1*). PCR amplification was performed in a volume of 20 μL using a LightCycler Nano (Roche) under the conditions suggested by the manufacturer. The results were normalized to S29 transcription as a housekeeping gene, which was comparable between the groups.

2.6 Statistical analysis

All data are presented as medians (interquartile ranges). Kruskal-Wallis and post-hoc Dunn's multiple comparison tests were used to compare the values among the three groups. The Wilcoxon or Friedman test was used to test repeated values. The Mann-Whitney U test was used to compare the values between the two groups; for the relevant magnitudes of the difference, the effect size was also calculated and considered a “large effect” when it was > 0.5. Spearman correlation coefficient (r) was computed in the correlation analysis between the two parameters. Differences were considered significant at $P < 0.05$. GraphPad Prism version 9.1.1 (GraphPad Software, San Diego, CA, USA) was used for statistical analysis.

3. Results

3.1 Cardiac functional parameters

Figure 1b-d shows the LV functional parameters. LVDd and wall stress were smaller in the

SVR group than in the sham group early after SVR, although the differences did not exist in the late phase (**Fig. 1b, d**). Fractional shortening, a systolic functional parameter, was smaller in the sham group than in the control group in both early and late after SVR (**Fig. 1c**). Overall, SVR had the effects of LV wall stress reduction, whereas the significance was lost due to LV redilation late after SVR.

Table 1 presents the body, heart, and lung weight, heart rate, and infarct size at each time point. These variables were comparable between sham and SVR groups. Heart weight was greater in SVR than in control owing to the large granulation tissues around the heart and felt sandwiches used for SVR.

3.2 Myocyte hypertrophy and myocardial fibrosis

Figure 2 shows the results of the histological examination 28 days after SVR. The myocyte area was larger in the sham group than in the control group, while it was comparable between the SVR and control groups (**Fig. 2a**). The fibrosis rate was also higher in the sham group than in the control group, while it was comparable between the SVR and control groups (**Fig. 2b**). These findings suggest that myocyte reverse remodeling occurs after SVR.

3.3 Autophagy markers, AKT, and AMPKα

Figure 3 shows the protein expression levels of the autophagy markers, AKT, and AMPKα. The protein expression of LC3-II, p62, and AKT phosphorylation rates were comparable between the groups (**Fig. 3a, b**). The total AMPKα, p-AMPKα, and AMPKα phosphorylation rates were significantly higher in the SVR group than in the sham group (effect size, 0.83

0.83, and 0.70, respectively) (**Fig. 3c**). Furthermore, these AMPKα-related parameters were negatively correlated with myocyte area (**Fig. 3d**); the strongest correlation was observed between p-AMPK and myocytes (r = −0.9273).

3.4 Ubiquitin ligases and ubiquitinated proteins

Figure 4 shows the gene expression of ubiquitin ligases and ubiquitin protein expression. The expression of muscle-specific ubiquitin ligase *Atrogin-1* (effect size, 0.76) was smaller in the SVR group than in the sham group; *Murf-1* expression also tended to be reduced by SVR (**Fig. 4a**). Furthermore, *Atrogin-1* and *Murf-1* were positively correlated with myocyte area. *Atrogin-1* levels also correlated with LV wall stress (r = 0.7599, P = 0.014). The protein expression of ubiquitin was lower in the SVR group than in the sham group (effect size, 0.63) (**Fig. 4b**) and correlated with *Atrogin-1* gene expression (r = 0.6575, P = 0.043). There were significant negative correlations between the expression of *Atrogin-1* and AMPKα-related markers, except for p-AMPKα/AMPKα (**Fig. 4c**) and between the expression of *Murf-1* and AMPKα-related parameters (**Fig. 4d**). The strongest correlation was observed between p-AMPKα/AMPKα and the expression of *Murf-1* (r = −0.8875). These results suggest that SVR reduced the UPS in the myocardium, which was inversely correlated with AMPKα activation.

4. Discussion

We demonstrated that myocyte reverse remodeling after SVR was associated with increased AMPKα and reduced UPS in the LV myocardium.

4.1 AMPK as an anti-hypertrophic protein

Increased phosphorylation of AMPKα at Ser485/491 and Thr172 is associated with pro-hypertrophic and anti-hypertrophic responses, respectively [12]. Pharmacological activation of AMPK has been reported to increase AMPKα phosphorylation at Thr172 and inhibit cardiac hypertrophy by pressure overload by blocking the signaling transduction pathways that are involved in cardiac growth [3]. In the present study, AMPKα phosphorylation was also negatively correlated with myocyte area. Because AKT phosphorylation was not significantly changed by SVR, the AKT pathway may not be related to myocyte reverse remodeling in this setting.

4.2 Possible mechanism of increased AMPKα-ubiquitination

In the present study, total AMPK, p-AMPK, and p-AMPK/AMPK were all elevated in the SVR group. Furthermore, there were strong negative correlations between AMPKα markers and the expression of *Murf-1*. To date, ubiquitination by a number of ubiquitin ligase (E3) complexes has been reported on AMPK isoforms α, β, and γ. They are known to regulate AMPK expression and/or activity in a wide variety of settings, including makorin ring finger protein 1 (MKRN1), cullin-RING 4A (CRL4A), and TRIM27 for AMPKα-subunit ubiquitination [13]. The most common role of ubiquitination is to target AMPK to the proteasome for degradation. Although there is no evidence of a counter-regulation of AMPKα by *Atrogin-1* and *MuRF-1*, it is possible that AMPK upstream regulation by *Atrogin-1* and *MuRF-1* is involved in the adaptive responses of the heart to loading conditions [14].

The causal relationship between AMPKα activation and the reduction of *Atrogin-1* and *MuRF-1* remains to be further determined.

4.3 Ubiquitin ligases in pathological hypertrophy

Adams et al. reported the elevation of *Atrogin-1* and *MuRF-1* in a rat model of chronic heart failure after MI [15]. Degradation of troponin-I through these ubiquitin ligases is correlated with contractile dysfunction. Furthermore, downregulation of *Atrogin-1* and *MuRF-1* reversed the contractile function and Ca handling. Usui et al. proposed that *Atrogin-1* mediates pathological hypertrophy due to pressure overload in mice through proteasomal degradation of IκB and subsequent stabilization of NF-κB [16]. They demonstrated that the downregulation of *Atrogin-1* inhibited cardiac hypertrophy. In humans, a correlation between preoperative LV mass and gene expression of *Atrogin-1* has been shown in aortic valve stenosis [17]. Collectively, muscle-specific ubiquitin ligases play an important role in pathological hypertrophy. Thus, the reduced gene expression of ubiquitin ligase after LV unloading by SVR in the present study may have contributed to myocyte reverse remodeling.

Although the LV unloading effects of SVR on cardiac function were lost in the late phase, the myocyte area was reduced to the level of the control. We speculate that the LV redilation was due to the elongation of the scar tissue around the SVR stitch but not the myocyte. Any measures preventing LV redilation would be beneficial for cardiac function after SVR.

5. Conclusions

In myocyte reverse remodeling after SVR, the total protein expression of AMPKα and phosphorylation rate increased in association with reduced gene expression of ubiquitin ligases. Further studies are necessary to examine the causal relationship between AMPKα and ubiquitin ligases in this setting.

Statements & Declarations

Funding

This work was partly supported by Japan Heart Foundation Research Grant 2015 [to Yasushige Shingu]; Mochida Memorial Foundation for Medical and Pharmaceutical Research 2016 [to Yasushige Shingu].

Competing interests

The authors have no relevant financial or non-financial interests to disclose.

Author Contributions

All authors contributed to the study conception and design. Material preparation, data collection and analysis were performed by Yasushige Shingu, Tetsuya Hieda, Satoshi Sugimoto, Hidetsugu Asai, and Tomoji Yamakawa. Manuscript revision was performed by Satoru Wakasa. The first draft of the manuscript was written by Yasushige Shingu and all authors commented on previous versions of the manuscript. All authors read and approved the final manuscript.

Ethics approval

All procedures were approved by the National University Corporation Hokkaido University Animal Research Committee and consistent with the Guide for the Care and Use of Laboratory Animals, published by the US National Institute of Health (NIH publication No. 85-23, revised 1996).

References

1. Frey N, Olson EN (2003) Cardiac hypertrophy: the good, the bad, and the ugly. Annu Rev Physiol 65:45-79. https://doi.org/10.1146/annurev.physiol.65.092101.142243

2. Dyck JR, Lopaschuk GD (2006) AMPK alterations in cardiac physiology and pathology: enemy or ally? J Physiol 574:95-112. https://doi.org/10.1113/jphysiol.2006.109389

3. Li HL, Yin R, Chen D, Liu D, Wang D, Yang Q, Dong YG (2007) Long-term activation of adenosine monophosphate-activated protein kinase attenuates pressure-overload-induced cardiac hypertrophy. J Cell Biochem 100:1086-1099. https://doi.org/10.1002/jcb.21197

4. Yamaguchi O, Taneike M, Otsu K (2012) Cooperation between proteolytic systems in cardiomyocyte recycling. Cardiovasc Res 96:46-52. https://doi.org/10.1093/cvr/cvs236

5. Matsui Y (2009) Overlapping left ventricular restoration. Circ J 73 Suppl A:A13-18.

6. Sugimoto S, Shingu Y, Doenst T, Yamakawa T, Asai H, Wakasa S, Matsui Y (2020) Autophagy during left ventricular redilation after ventriculoplasty: Insights from a rat model of ischemic cardiomyopathy. J Thorac Cardiovasc Surg. 163:e33-e40. https://doi.org/10.1016/j.jtcvs.2020.01.080

7. Reichek N, Wilson J, St John Sutton M, Plappert TA, Goldberg S, Hirshfeld JW (1982) Noninvasive determination of left ventricular end-systolic stress: validation of the method and initial application. Circulation 65:99-108.

8. Thomson DM (2018) The Role of AMPK in the Regulation of Skeletal Muscle Size, Hypertrophy, and Regeneration. Int J Mol Sci 19:3125.

https://doi.org/10.3390/ijms19103125

9. Nave BT, Ouwens M, Withers DJ, Alessi DR, Shepherd PR (1999) Mammalian target of rapamycin is a direct target for protein kinase B: identification of a convergence point for opposing effects of insulin and amino-acid deficiency on protein translation. Biochem J 344 Pt 2:427-431.

10. Mizushima N, Yoshimori T, Levine B (2010) Methods in mammalian autophagy research. Cell 140:313-326. https://doi.org/10.1016/j.cell.2010.01.028

11. Lee D, Goldberg A (2011) Atrogin1/MAFbx: what atrophy, hypertrophy, and cardiac failure have in common. Circ Res 109:123-126. https://doi.org/10.1161/CIRCRESAHA.111.248872

12. Pang T, Rajapurohitam V, Cook MA, Karmazyn M (2010) Differential AMPK phosphorylation sites associated with phenylephrine vs. antihypertrophic effects of adenosine agonists in neonatal rat ventricular myocytes. Am J Physiol Heart Circ Physiol 298:H1382-1390. https://doi.org/10.1152/ajpheart.00424.2009

13. Ovens AJ, Scott JW, Langendorf CG, Kemp BE, Oakhill JS, Smiles WJ (2021) Post-Translational Modifications of the Energy Guardian AMP-Activated Protein Kinase. Int J Mol Sci 22:1229. https://doi.org/10.3390/ijms22031229

14. Zungu M, Schisler JC, Essop MF, McCudden C, Patterson C, Willis MS (2011) Regulation of AMPK by the ubiquitin proteasome system. Am J Pathol 178:4-11. https://doi.org/10.1016/j.ajpath.2010.11.030

15. Adams V, Linke A, Wisloff U, Doring C, Erbs S, Krankel N, Witt CC, Labeit S, Muller-Werdan U, Schuler G, Hambrecht R (2007) Myocardial expression of Murf-1 and MAFbx after induction of chronic heart failure: Effect on myocardial contractility. Cardiovasc Res 73:120-129. https://doi.org/10.1016/j.cardiores.2006.10.026

16. Usui S, Maejima Y, Pain J, Hong C, Cho J, Park JY, Zablocki D, Tian B, Glass DJ, Sadoshima J (2011) Endogenous muscle atrophy F-box mediates pressure overload-induced cardiac hypertrophy through regulation of nuclear factor-kappaB. Circ Res 109:161-171. https://doi.org/10.1161/CIRCRESAHA.110.238717

17. Trindade F, Saraiva F, Keane S, Leite-Moreira A, Vitorino R, Tajsharghi H, Falcao-Pires I (2020) Preoperative myocardial expression of E3 ubiquitin ligases in aortic stenosis patients undergoing valve replacement and their association to postoperative hypertrophy. PLoS One 15:e0237000. https://doi.org/10.1371/journal.pone.0237000

Figure legends

Fig. 1 Study protocol (**a**) and cardiac functional parameters at baseline, pre SVR, early (2 days), and late (28 days) after SVR (**b**: LVDd; **c**: FS; **d**: wall stress). The numbers of rats were 5 for each group. *P < 0.05, **P < 0.01, ***P < 0.001. $^{\#}$P < 0.05, $^{\#\#}$P < 0.01 vs. baseline. ctrl, control; FS, fractional shortening; LVDd, left ventricular end-diastolic dimension; ns, not significant; SVR, surgical ventricular reconstruction.

Fig. 2 Hematoxylin-eosin (**a**) and Masson's trichrome staining (**b**) at the mid-ventricular level 28 days after SVR. The numbers of rats were 5 for each group. *P < 0.05.**P < 0.01. ctrl, control; SVR, surgical ventricular reconstruction.

Fig. 3 Protein expressions of autophagy markers, AKT, and AMPKα. (**a**) Representative bands and quantitative analysis of LC3-II and p62. (**b**) Representative bands and quantitative analysis of p-AKT / AKT; (**c**) Representative bands and quantitative analysis of total AMPKα, p-AMPKα, and p-AMPKα / AMPKα. (**d**) Correlation between AMPKα-related parameters and myocyte area. The numbers of rats were 5 for each group. *P < 0.05, **P < 0.01. AMPKα, adenosine monophosphate-activated protein kinase α; p-AMPKα, phospho-AMPKα (Thr172); GAPDH, glyceraldehyde-3-phosphate dehydrogenase; LC3, microtubule-associated protein light chain 3; ns, not significant; SVR, surgical ventricular reconstruction.

Fig. 4 Gene expression of ubiquitin ligases and protein expression of Ubiquitin. (**a)** Gene expressions of ubiquitin ligases (left) and the correlations with myocyte area (right). **(b)** Bands and quantitative analysis of protein expression of Ubiquitin. **(c)** Correlations

between the expression of *Atrogin-1* and the AMPKα-related parameters. **(d)** Correlations between the expression of *Murf-1* and the AMPKα-related parameters. The numbers of rats were 5 for each group. *P < 0.05. AMPKα, adenosine monophosphate-activated protein kinase α; SVR, surgical ventricular reconstruction.

Table 1. Body, heart, and lung weights, heart rate, and scar ratio

Time points (age)	Baseline (10 w)			Pre SVR (14 w)			2 days (14 w)			28 days (18 w)		
	ctrl	sham	SVR	ctrl	sham	SVR	ctrl	sham	SVR	ctrl	sham	SVR
Body weight, g	338 (22)	340 (28)	347 (21)	448 (45)	429 (29)	440 (55)	463 (28)	400 (38)*	394 (75)*	500 (65)	460 (60)	430 (145)
Heart rate, bpm	330 (45)	307 (59)	305 (21)	297 (48)	261 (35)**	278 (46)	291 (49)	297 (71)	303 (48)	287 (94)	261 (43)	298 (53)
Heart weight, g	NA	NA	NA	NA	NA	NA	1.0 (0.2)	1.2 (0.2)	1.4 (0.2)**	1.1 (0.2)	1.4 (0.2)	2.2 (1.4)**
Lung weight, g	NA	NA	NA	NA	NA	NA	1.5 (0.2)	1.7 (0.6)	2.9 (1.5)	1.5 (0.2)	2.0 (0.9)*	2.0 (1.7)*
Scar ratio, %	NA	NA	NA	NA	33 (7)	36 (5)	NA	NA	NA	NA	NA	NA

Values are median (Interquartile range). *P < 0.05, **P < 0.01 vs. ctrl. ctrl, control; NA, not applicable; SVR, surgical ventricular reconstruction.

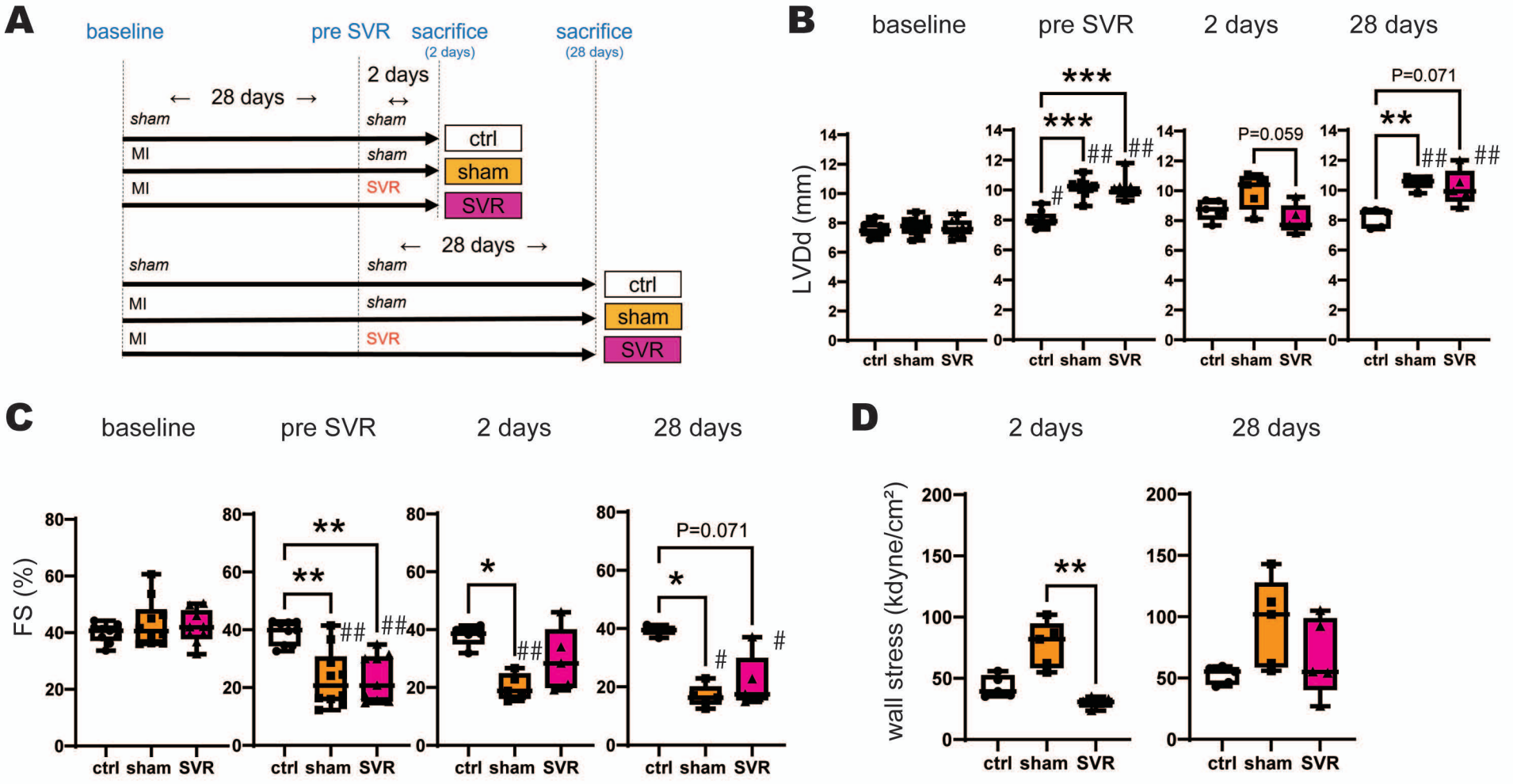
A
baseline
pre SVR
sacrifice (2 days)
sacrifice (28 days)
2 days
28 days
sham
MI
SVR
ctrl
sham
SVR
B
baseline
pre SVR
2 days
28 days
LVDd (mm)
***
**
P=0.059
P=0.071
ctrl sham SVR
C
baseline
pre SVR
2 days
28 days
FS (%)
**
*
P=0.071
ctrl sham SVR
D
2 days
28 days
wall stress (kdyne/cm²)
**
ctrl sham SVR

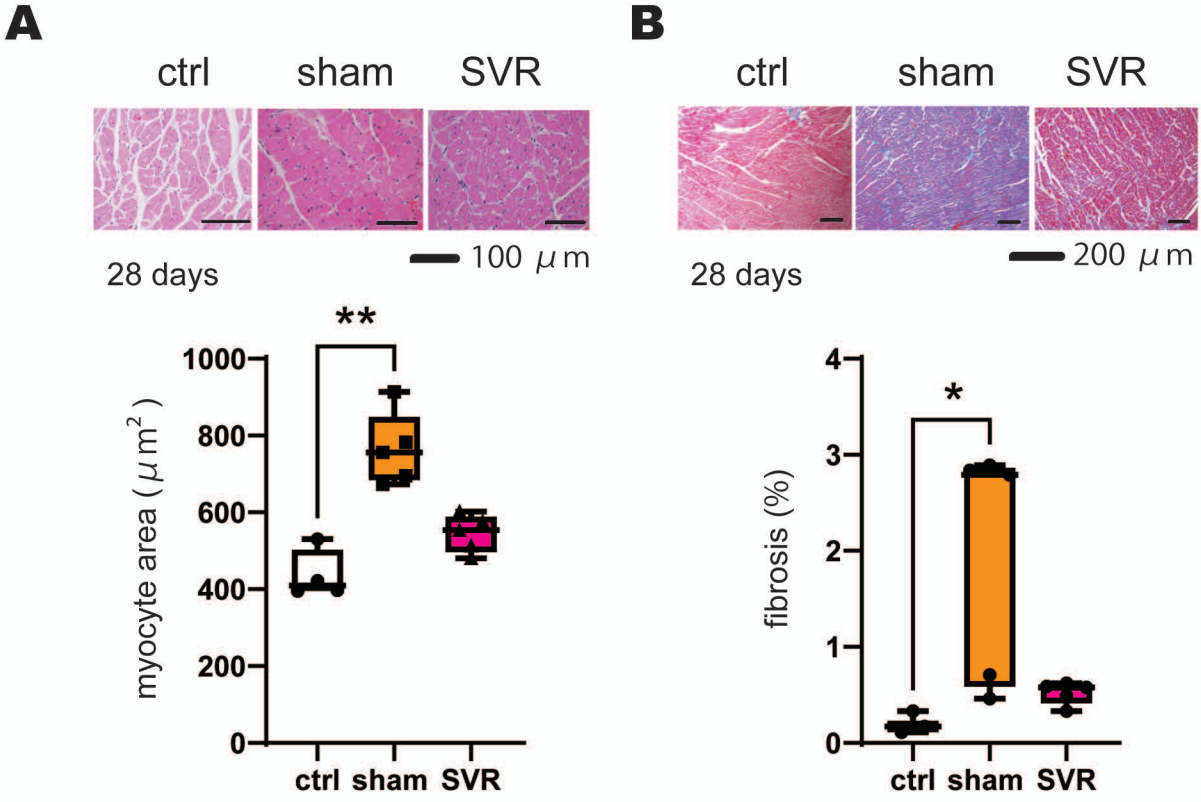
A
ctrl
sham
SVR
100 μm
28 days
**
myocyte area (μm²)
1000
800
600
400
200
0
ctrl
sham
SVR
B
ctrl
sham
SVR
200 μm
28 days
*
fibrosis (%)
4
3
2
1
0
ctrl
sham
SVR

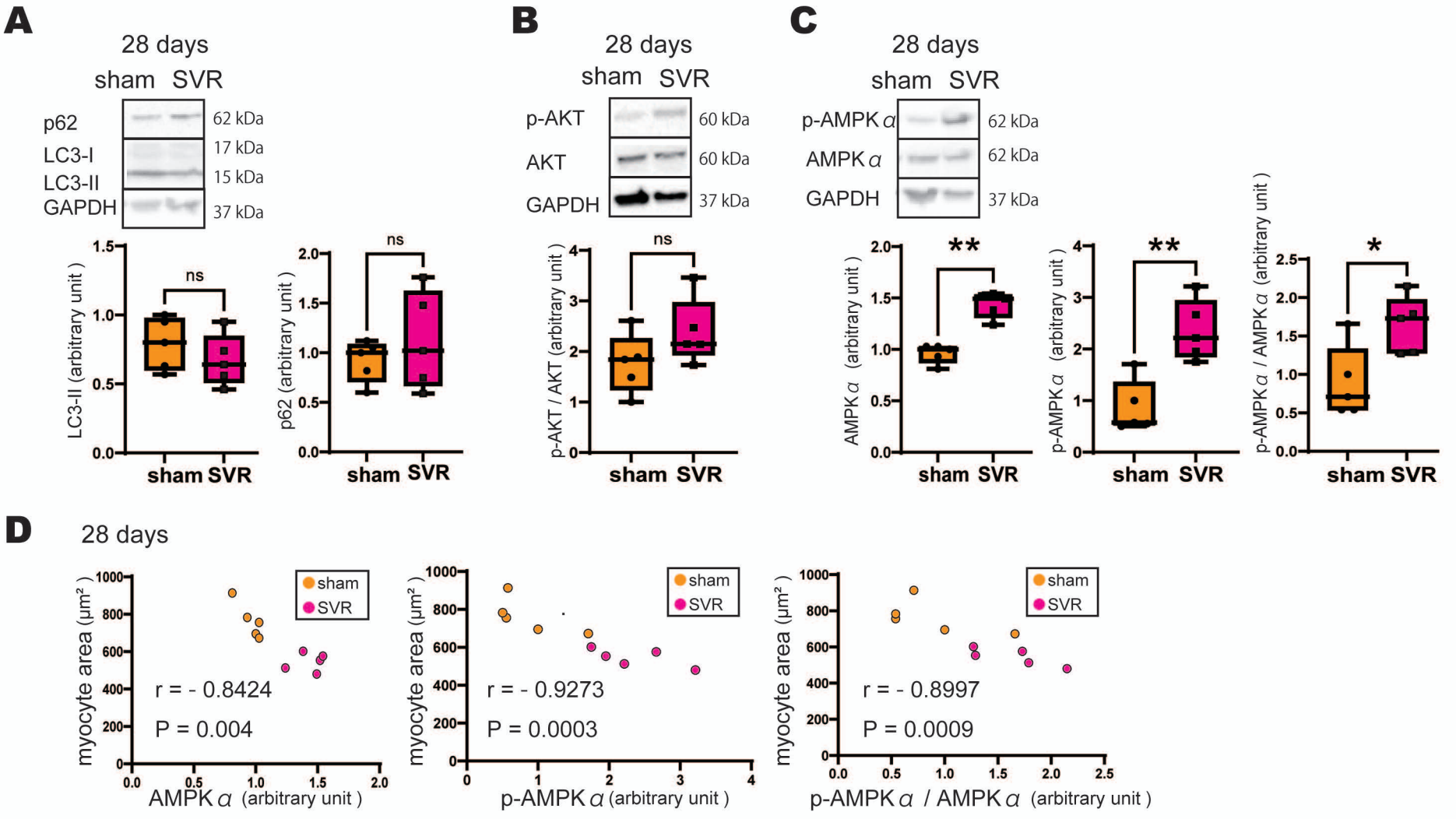
A
28 days
sham SVR
p62
LC3-I
LC3-II
GAPDH
62 kDa
17 kDa
15 kDa
37 kDa
LC3-II (arbitrary unit)
p62 (arbitrary unit)
ns
sham SVR
B
28 days
sham SVR
p-AKT
AKT
GAPDH
60 kDa
60 kDa
37 kDa
p-AKT / AKT (arbitrary unit)
C
28 days
sham SVR
p-AMPK α
AMPK α
GAPDH
62 kDa
62 kDa
37 kDa
AMPK α (arbitrary unit)
p-AMPK α (arbitrary unit)
p-AMPK α / AMPK α (arbitrary unit)
**
*
D
28 days
sham
SVR
myocyte area (μm²)
r = - 0.8424
P = 0.004
AMPK α (arbitrary unit)
r = - 0.9273
P = 0.0003
p-AMPK α (arbitrary unit)
r = - 0.8997
P = 0.0009
p-AMPK α / AMPK α (arbitrary unit)

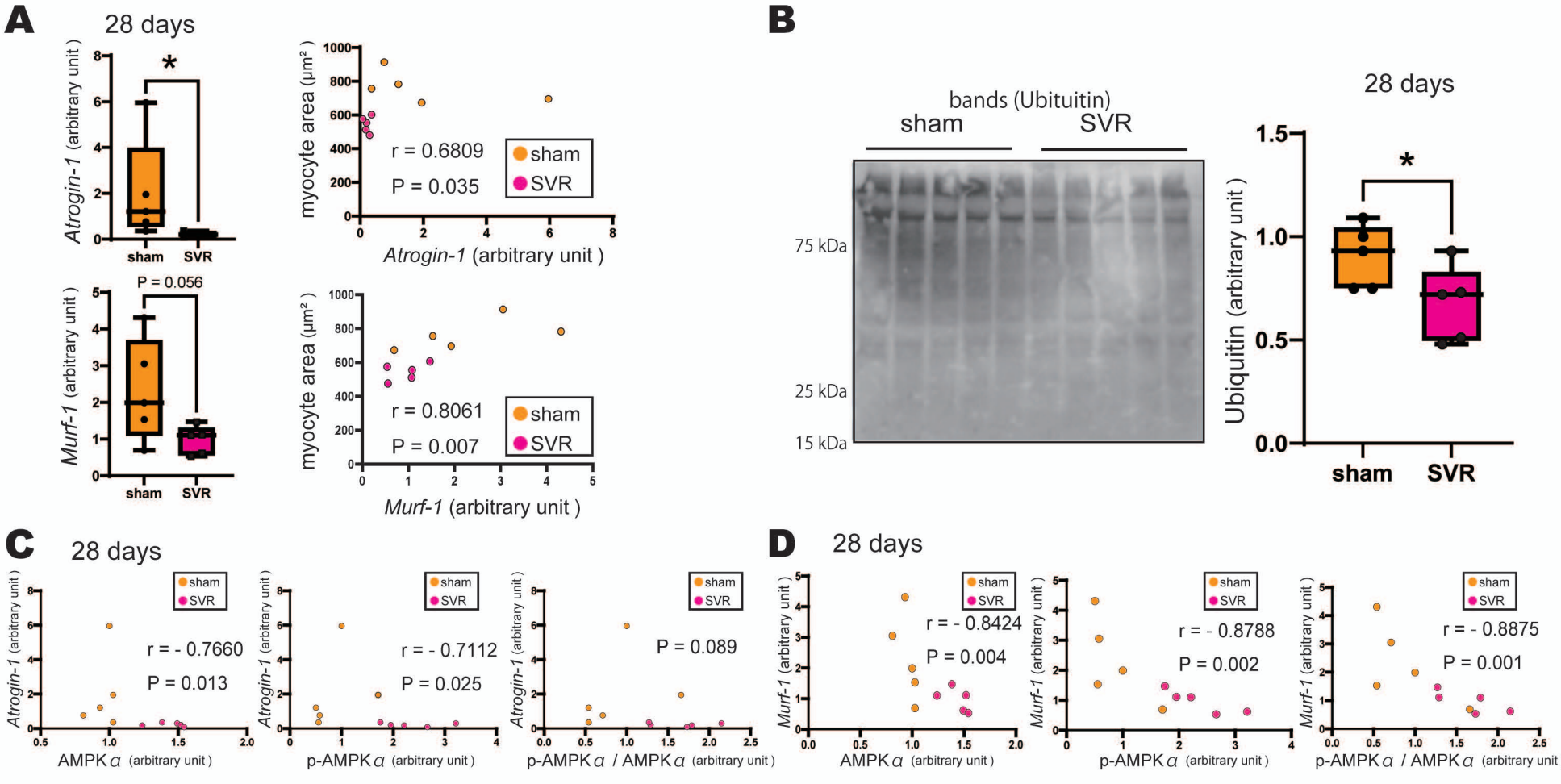
A
28 days
Atrogin-1 (arbitrary unit)
*
sham
SVR
P = 0.056
Murf-1 (arbitrary unit)
myocyte area (μm²)
r = 0.6809
P = 0.035
sham
SVR
Atrogin-1 (arbitrary unit)
r = 0.8061
P = 0.007
Murf-1 (arbitrary unit)
B
bands (Ubituitin)
sham
SVR
75 kDa
25 kDa
15 kDa
28 days
Ubiquitin (arbitrary unit)
C
28 days
r = - 0.7660
P = 0.013
AMPK α (arbitrary unit)
r = - 0.7112
P = 0.025
p-AMPK α (arbitrary unit)
P = 0.089
p-AMPK α / AMPK α (arbitrary unit)
D
28 days
r = - 0.8424
P = 0.004
r = - 0.8788
P = 0.002
r = - 0.8875
P = 0.001